Coupled Systems Mechanics, *Vol. 10, No. 5 (2021) 453-467*
https://doi.org/10.12989/csm.2021.10.5.453

Distributed loads in modified couple stress thermoelastic diffusion with non-local and phase-lags

Rajneesh Kumar[1], Sachin Kaushal*[2] and Vikram Dahiya[2]

[1]*Department of Mathematics, Kurukshetra University, Kurukshetra-136119 Haryana, India*
[2]*Department of Mathematics, School of Chemical Engineering and Physical Sciences, Lovely Professional University-144411 Phagwara, India*

(Received April 27, 2021, Revised June 19, 2021, Accepted October 6, 2021)

Abstract. Thermomechanical loading is considered to examine the non-local and phase-lags effects in a modified couple stress thermoelastic (MCT) half space. Governing equations are solved by using Laplace and Fourier transform techniques. Concentrated source in time and distributed sources with space variable are taken to demonstrate the application. Distributed sources are further classified as uniformly distributed source (UDS) and linearly distributed source (LDS) for mechanical, thermal and chemical potential sources. Numerical results are calculated for displacements, stresses, temperature distribution and chemical potential and are disucussed by displaying graphically. Some particular cases are deduced.

Keywords: dual-phase-lag; Laplace and Fourier transforms; LDS; modified couple stress thermoelasticity; non-local; UDS

1. Introduction

The state of stress at a point is a function of strain of all points in the body for non-local theory of elasticity, whereas classical (local) elasticity describes the stress state at a given point by strain state at the same point. Non-local theory has been derived by various researchers by adopting different assumptions, e.g., Eringen and Edelen (1972), Edelen and Law (1971), Eringen (1972a, 1972b, 1981, 1991). A comprehensive work on development of non-local theory is given by book of Eringen (2002).

The non-local response and lagging response are same since earlier in space and as later in time. Tzou (1992) combined the response of non-local with single phase-lag heat conduction and compared it with the model given by Cao and Guo (2007), Guo and Hou (2010). Tzou and Guo (2010) demonstrate the union of non-local response with the dual-phase-lag model proposed by Tzou (1995a, 1995b) and known as the new theory comprising both effects.

Sharma (2012) studied reflection of plane waves in thermodiffusive elastic half space with voids. Abouelregal and Zenkour (2014) analyzed the effect of phase lags on thermoelastic functionally graded microbeams subjected to ramp-type heating. Sharma *et al*. (2014) investigated the influence of heat sources and relaxation time on temperature distribution in tissues. Marin *et al*. (2014) studied

*Corresponding author, Ph.D., E-mail: sachin_kuk@yahoo.co.in

http://www.techno-press.org/?journal=csm&subpage=8 ISSN: 2234-2184 (Print), 2234-2192 (Online)

relaxed Saint-Venant principle for thermoelastic micropolar diffusion. Kumar and Abbas (2016) studied the disturbance due to thermomechanical sources in porothermoelastic medium. Abbas and Marin (2018) investigated analytical solution for two dimensional generalised thermoelastic diffusion problem.

Kumar *et al*. (2018) investigated transient analysis of non-local microstretch thermoelastic thick circular plate with phase-lags. Kumar *et al*. (2019) studied the effect of thermal and chemical potential sources in a thin beam in MCT with three-phase-lag thermoelastic diffusion model. Zhang *et al*. (2020) studied entropy generation on blood flow through anisotropic tapered arteries filled with magnetic zinc oxide nanoparticles. Borjalilou *et al*. (2020) investigated an explicit relation for thermoelastic damping in non-local nanobeams considering dual-phase-lag effect. Mashat and Zenkour (2020) presented a problem of ramp-type heating to study vibration of a temperature dependent nanobeam under multi-dual-phase-lag thermoelastic with non-local.

In this article, non-local and phase-lags effects are examined due to distributed sources in MCT diffusion. Integral transform technique is applied to investigate the problem. Normal load, thermal source and chemical potential source are taken to show the approach. Resulting quantities are depicted graphically to show non-local and phase-lags effects. This theory can help to capture the size effect of elastic deformation and heat conduction of nanoscale structures with thermal lagging which can be useful in nanotechnology.

2. Basic equations

Following Tzou and Guo (2010), Sherief *et al*. (2004) and Yu *et al*. (2016), we have

(i) Constitutive Relations

$$t_{ij} = 2\mu e_{ij} - \frac{1}{2} e_{kij} m_{lk,l} + \delta_{ij}[\lambda_0 e_{kk} - \gamma_1 T - \gamma_2 P], \tag{1}$$

$$m_{ij} = 2\alpha \chi_{ij}, \tag{2}$$

(ii) Equation of motion

$$(\lambda_0 + \mu + \frac{\alpha}{4}\Delta)\nabla(\nabla \cdot \vec{u}) + (\mu - \frac{\alpha}{4}\Delta)(\Delta \vec{u}) - \gamma_1 \nabla T - \gamma_2 \nabla P = \rho(1 - \xi^2 \Delta)\frac{\partial^2 \vec{u}}{\partial t^2}, \tag{3}$$

(iii) Equation of heat conduction

$$(1 - \zeta^2 \Delta + \tau_q \frac{\partial}{\partial t} + \frac{1}{2}\tau_q^2 \frac{\partial^2}{\partial t^2})(\gamma_1 T_0 \dot{e} + l_1 T_0 \dot{T} + T_0 d\dot{P}) = K(1 + \tau_t \frac{\partial}{\partial t})\Delta T, \tag{4}$$

(iv) Equation of mass diffusion

$$(1 - \varsigma^2 \Delta + \tau_u \frac{\partial}{\partial t} + \frac{1}{2}\tau_u^2 \frac{\partial^2}{\partial t^2})(\gamma_2 \dot{e} + d\dot{T} + n\dot{P}) = D(1 + \tau_p \frac{\partial}{\partial t})\Delta P, \tag{5}$$

Here

$$\chi_{ij} = \frac{1}{2}(\omega_{i,j} + \omega_{j,i}), \omega_i = \frac{1}{2} e_{ipq} u_{q,p}$$

where

$$\lambda_o = \lambda - \frac{\beta_2^2}{b},\ \gamma_1 = \beta_1 + \frac{a}{b}\beta_2,\ \gamma_2 = \frac{\beta_2}{b},\ l_1 = \frac{\rho C_e}{T_o} + \frac{a^2}{b},\ d = \frac{a}{b},\ n = \frac{1}{b}\ .$$

In the Eqs. (1)-(5), ξ, ζ, ς - non-local parameters, $\tau_q \& \tau_t$ - thermal relaxation times with $\tau_q, \tau_t \geq 0$ and $\tau_u \& \tau_p$ - diffusion relaxation times with $\tau_u, \tau_p \geq 0$. $\beta_1 = (3\lambda + 2\mu)\alpha_t$, $\beta_2 =$

$(3\lambda + 2\mu)\alpha_c$. Here α_t, α_c correspond to the coefficient of linear thermal expansion and diffusion expansion respectively. Δ is the Laplacian operator, ∇ is nabla(gradient) operator. Other symbols have their usual meanings.

3. Statement of the problem

A homogeneous isotropic non-local MCT diffusive body with dual-phase-lag occupying the region $x_3 \geq 0$ is taken. A rectangular Cartesian coordinate system (x_1, x_2, x_3) having origin on $x_3 = 0$ is followed. The half space is subjected to normal load, thermal source and chemical potential source on the bounding plane $x_3 = 0$.

For the assumed model, we have

$$\vec{u} = (u_1(x_1, x_3, t), 0, u_3(x_1, x_3, t)), T(x_1, x_3, t), P(x_1, x_3, t). \tag{6}$$

Using Eqs. (6) in (3)-(5), recast the following equations

$$(\lambda_o + \mu)\frac{\partial e}{\partial x_1} + \mu \Delta u_1 + \frac{\alpha}{4}\Delta\left(\frac{\partial e}{\partial x_1} - \Delta u_1\right) - \gamma_1 \frac{\partial T}{\partial x_1} - \gamma_2 \frac{\partial P}{\partial x_1} = \rho(1 - \xi^2 \Delta)\frac{\partial^2 u_1}{\partial t^2}, \tag{7}$$

$$(\lambda_o + \mu)\frac{\partial e}{\partial x_3} + \mu \Delta u_3 + \frac{\alpha}{4}\Delta\left(\frac{\partial e}{\partial x_3} - \Delta u_3\right) - \gamma_1 \frac{\partial T}{\partial x_3} - \gamma_2 \frac{\partial P}{\partial x_3} = \rho(1 - \xi^2 \Delta)\frac{\partial^2 u_3}{\partial t^2}, \tag{8}$$

$$(1 - \zeta^2 \Delta + \tau_q \frac{\partial}{\partial t} + \frac{1}{2}\tau_q^2 \frac{\partial^2}{\partial t^2})(\gamma_1 T_o \dot{e} + l_1 T_o \dot{T} + T_o d\dot{P}) = K(1 + \tau_t \frac{\partial}{\partial t})\Delta T, \tag{9}$$

$$(1 - \varsigma^2 \Delta + \tau_u \frac{\partial}{\partial t} + \frac{1}{2}\tau_u^2 \frac{\partial^2}{\partial t^2})(\gamma_2 \dot{e} + d\dot{T} + n\dot{P}) = D(1 + \tau_p \frac{\partial}{\partial t})\Delta P \tag{10}$$

Following dimensionless quantities are used

$$\begin{aligned}
&\xi' = \frac{\omega^*}{c_1}\xi, \qquad \zeta' = \frac{\omega^*}{c_1}\zeta, \qquad \varsigma' = \frac{\omega^*}{c_1}\varsigma, \qquad x_i' = \frac{\omega^*}{c_1}x_i, \qquad u_i' = \frac{\omega^*}{c_1}u_i, \\
&t' = \omega^* t, \qquad \tau_t' = \omega^* \tau_t, \qquad \tau_q' = \omega^* \tau_q, \qquad \tau_u' = \omega^* \tau_u, \qquad \tau_p' = \omega^* \tau_p, \\
&t_{ij}' = \frac{1}{\gamma_1 T_o} t_{ij}, \quad m_{ij}' = \frac{\omega^*}{\gamma_1 T_o c_1} m_{ij}, \qquad T' = \frac{\gamma_1}{\rho c_1^2} T, \quad P' = \frac{1}{b\gamma_2} P
\end{aligned} \tag{11}$$

where $\omega^* = \frac{\rho C_e c_1^2}{K}, c_1^2 = \frac{\lambda_o + 2\mu}{\rho}$.

ω^* is the characteristic frequency and c_1 is the longitudinal wave velocity in the media.

Eqs. (7)-(10) with the aid of Eq. (11), reduce to the following equations after suppressing the primes

$$a_1 \frac{\partial e}{\partial x_1} + a_2 \Delta u_1 + a_3 \Delta\left(\frac{\partial e}{\partial x_1} - \Delta u_1\right) - \frac{\partial T}{\partial x_1} - a_4 \frac{\partial P}{\partial x_1} = (1 - \xi^2 \Delta)\frac{\partial^2 u_1}{\partial t^2}, \tag{12}$$

$$a_1 \frac{\partial e}{\partial x_3} + a_2 \Delta u_3 + a_3 \Delta\left(\frac{\partial e}{\partial x_3} - \Delta u_3\right) - \frac{\partial T}{\partial x_3} - a_4 \frac{\partial P}{\partial x_3} = (1 - \xi^2 \Delta)\frac{\partial^2 u_3}{\partial t^2}, \tag{13}$$

$$(1-\zeta^2\Delta+\tau_q\frac{\partial}{\partial t}+\frac{1}{2}\tau_q^2\frac{\partial^2}{\partial t^2})(a_5\dot{e}+a_6\dot{T}+a_7\dot{P})=(1+\tau_t\frac{\partial}{\partial t})\Delta T, \tag{14}$$

$$(1-\varsigma^2\Delta+\tau_u\frac{\partial}{\partial t}+\frac{1}{2}\tau_u^2\frac{\partial^2}{\partial t^2})(a_8\dot{e}+a_9\dot{T}+a_{10}\dot{P})=(1+\tau_p\frac{\partial}{\partial t})\Delta P\ . \tag{15}$$

where

$$a_1=\frac{(\lambda_o+\mu)}{\rho c_1^2},\quad a_2=\frac{\mu}{\rho c_1^2},\quad a_3=\frac{\alpha}{4}\frac{\omega^{*^2}}{\rho c_1^4},\quad a_4=\frac{b\gamma_2^2}{\rho c_1^2},\quad a_5=\frac{\gamma_1^2}{K\rho\omega^*}T_o,\quad a_6=\frac{l_1c_1^2}{K\omega^*}T_o,$$

$$a_7=\frac{b\gamma_2\gamma_1T_od}{K\rho\omega^*},\quad a_8=\frac{c_1^2}{Db\omega^*},\quad a_9=\frac{c_1^4d\rho}{Db\omega*\gamma_1\gamma_2},\quad a_{10}=\frac{nc_1^2}{D\omega^*},\quad \Delta=\frac{\partial^2}{\partial x_1^2}+\frac{\partial^2}{\partial x_3^2},\quad e=\frac{\partial u_1}{\partial x_1}+\frac{\partial u_3}{\partial x_3}.$$

4. Solution procedure

Following Helmholtz's decomposition, the displacement components $u_1(x_1,x_3,t)$ and $u_3(x_1,x_3,t)$ relate to scalar potentials $\varphi(x_1,x_3,t)$ and $\psi(x_1,x_3,t)$ in dimensionless form as

$$u_1=\frac{\partial\varphi}{\partial x_1}+\frac{\partial\psi}{\partial x_3},u_3=\frac{\partial\varphi}{\partial x_3}-\frac{\partial\psi}{\partial x_1}. \tag{16}$$

With the aid of Eq. (16), Eqs. (12)-(15) yield

$$(a_1+a_2)\Delta\varphi-T-a_4P-(1-\xi^2\Delta)\frac{\partial^2\varphi}{\partial t^2}=0, \tag{17}$$

$$(a_2-a_3\Delta)\Delta\psi-(1-\xi^2\Delta)\frac{\partial^2\psi}{\partial t^2}=0, \tag{18}$$

$$(1-\zeta^2\Delta+\tau_q\frac{\partial}{\partial t}+\frac{1}{2}\tau_q^2\frac{\partial^2}{\partial t^2})(a_5\Delta\dot{\varphi}+a_6\dot{T}+a_7\dot{P})=(1+\tau_t\frac{\partial}{\partial t})\Delta T, \tag{19}$$

$$(1-\varsigma^2\Delta+\tau_u\frac{\partial}{\partial t}+\frac{1}{2}\tau_u^2\frac{\partial^2}{\partial t^2})(a_8\Delta\dot{\varphi}+a_9\dot{T}+a_{10}\dot{P})=(1+\tau_p\frac{\partial}{\partial t})\Delta P, \tag{20}$$

We define Laplace and Fourier transforms as

$$\overline{f}(x_1,x_3,s)=\int_0^\infty f(x_1,x_3,t)e^{-st}dt,$$
$$\hat{f}(\xi_1,x_3,s)=\int_{-\infty}^{\infty}\overline{f}(x_1,x_3,s)e^{i\xi_1x_1}dx_1. \tag{21}$$

Using Eq. (21) on Eqs. (17)-(20), determines following after simplification

$$(W_1D_1^6+W_2D_1^4+W_3D_1^2+W_4)(\hat{\varphi},\hat{T},\hat{P})=0, \tag{22}$$

$$(D_1^4+W_5D_1^2+W_6)\hat{\psi}=0. \tag{23}$$

where

$$W_1=W_{11}W_{13}W_{15}-a_7a_9s^2W_{11}\zeta^2\varsigma^2-a_5sW_{15}\zeta^2+a_7a_8s^2\zeta^2\varsigma^2-a_4a_5a_9s^2\zeta^2\varsigma^2+a_4a_8sW_{13}\varsigma^2,$$
$$W_2=W_{01}-3\xi_1^2W_1,W_3=3\xi_1^4W_1-2\xi_1^2W_{01}+W_{02},W_4=W_{01}\xi_1^4-W_1\xi_1^6-W_{02}\xi_1^2-W_{03},$$
$$W_5=-\frac{a_2+\xi^2s^2+2\xi_1^2a_3}{a_3},W_6=\frac{a_3\xi_1^4+a_2\xi_1^2+s^2+\xi_1^2\xi^2s^2}{a_3},$$

$$W_{01} = -W_{11}W_{22}W_{15} - W_{11}W_{13}W_{26} - W_{13}W_{15}s^2 + a_7sW_{11}W_{25}\zeta^2 + a_9sW_{23}W_{11}\varsigma^2 + a_7a_9\zeta^2\varsigma^2s^4 + a_5sW_{26}\zeta^2 + W_{21}W_{15} - a_7sW_{24}\zeta^2 - a_8sW_{23}\varsigma^2 + a_5sW_{24}a_4\zeta^2 + a_9sW_{21}a_4\varsigma^2 - W_{13}W_{24}a_4 - a_8sW_{22}\varsigma^2a_4, W_{02} = W_{11}W_{22}W_{26} + W_{13}W_{26}s^2 + W_{22}W_{15}s^2 - W_{11}W_{23}W_{25} - a_7W_{25}\zeta^2s^3 - a_9W_{23}\varsigma^2s^3 - W_{21}W_{26} + W_{23}W_{24} - W_{21}W_{25}a_4 + W_{22}W_{24}a_4, W_{03} = -s^2W_{26}W_{22} + s^2W_{23}W_{25},$$

$$W_{11} = a_1 + a_2 + \xi^2s^2, W_{12} = 1 + s\tau_q + \frac{s^2}{2}\tau_q^2, W_{13} = a_6s\zeta^2 + 1 + s\tau_t, W_{14} = 1 + s\tau_u + \frac{s^2}{2}\tau_u^2,$$

$$W_{15} = 1 + s\tau_p + s\zeta^2a_{10}, W_{21} = a_5sW_{12}, W_{22} = a_6sW_{12}, W_{23} = a_7sW_{12}, W_{24} = a_8sW_{14},$$

$$W_{25} = a_9sW_{14}, W_{26} = a_{10}sW_{14}.$$

The bounded solution of Eq. (22) and Eq. (23) are

$$(\hat{\varphi}, \hat{T}, \hat{P})(x_3, \xi_1, s) = \sum_{i=1}^{3}(1, R_i^*, S_i^*)A_i\, e^{-m_ix_3}, \tag{24}$$

$$\hat{\psi}(x_3, \xi_1, s) = \sum_{i=4}^{5} A_i\, e^{-m_ix_3}. \tag{25}$$

Here $m_i (i = 1,2,\ldots,5)$ are the roots of Eq. (22) and Eq. (23) and the coupling constants are given by

$$R_i^* = \frac{(m_i^2-\xi_1^2)^3(a_7sW_{34}\zeta^2\varsigma^2 - a_5sW_{15}\zeta^2) + (m_i^2-\xi_1^2)^2(a_5sW_{26}\zeta^2 + W_{21}W_{15} - a_7sW_{24}\zeta^2 - a_9sW_{21}\varsigma^2) + (m_i^2-\xi_1^2)(W_{21}W_{25} - W_{23}W_{24})}{(m_i^2-\xi_1^2)^2(W_{13}W_{15} - a_7a_9s^2\zeta^2\varsigma^2) + (m_i^2-\xi_1^2)(-W_{22}W_{15} - W_{13}W_{26} + a_7sW_{25}\zeta^2 + a_9sW_{23}\varsigma^2) + (W_{22}W_{26} - W_{23}W_{25})},$$

$$S_i^* = \frac{(m_i^2-\xi_1^2)^3(a_5a_9s^2\zeta^2\varsigma^2 - a_8sW_{13}\varsigma^2) + (m_i^2-\xi_1^2)^2(a_8sW_{22}\varsigma^2 + W_{13}W_{24} - a_5sW_{25}\zeta^2 - a_9sW_{21}\varsigma^2) + (m_i^2-\xi_1^2)(W_{21}W_{25} - W_{22}W_{24})}{(m_i^2-\xi_1^2)^2(W_{13}W_{15} - a_7a_9s^2\zeta^2\varsigma^2) + (m_i^2-\xi_1^2)(-W_{22}W_{15} - W_{13}W_{26} + a_7sW_{25}\zeta^2 + a_9sW_{23}\varsigma^2) + (W_{22}W_{26} - W_{23}W_{25})}, \qquad i = 1,2,3.$$

5. Thermomechanical conditions

Boundary conditions for plane boundary $x_3 = 0$ subjected to normal force, thermal source and chemical potential source are

$$t_{33} = -F_1(x_1)\delta(t), t_{31} = 0, m_{32} = 0, T = F_2(x_1)\delta(t), P = F_3(x_1)\delta(t). \tag{26}$$

Non dimensional stress components are given by

$$t_{33} = 2r_1\left(\frac{\partial u_3}{\partial x_3}\right) + r_2\left(\frac{\partial u_1}{\partial x_1} + \frac{\partial u_3}{\partial x_3}\right) - r_3T - r_4P, \tag{27}$$

$$t_{31} = r_1\left(\frac{\partial u_1}{\partial x_3} + \frac{\partial u_3}{\partial x_1}\right) - r_5\Delta\left(\frac{\partial u_1}{\partial x_3} - \frac{\partial u_3}{\partial x_1}\right), \tag{28}$$

$$m_{32} = 2r_5\frac{\partial}{\partial x_3}\left(\frac{\partial u_1}{\partial x_3} - \frac{\partial u_3}{\partial x_1}\right). \tag{29}$$

Using Eq. (21) on Eq. (26), we get

$$\hat{t}_{33} = -\hat{F}_1(\xi_1), \hat{t}_{31} = 0, \hat{m}_{32} = 0, \hat{T} = \hat{F}_2(\xi_1), \hat{P} = \hat{F}_3(\xi_1). \tag{30}$$

Making use of Eq. (24) and Eq. (25) in Eq. (30) along with Eq. (16), Eq. (21) and Eqs. (27)-(29) we get

$$\widehat{u}_1 = -\frac{i\xi_1}{\Delta}\sum_{i=1}^{3}\Delta_i e^{-m_i x_3} + \frac{1}{\Delta}\sum_{i=4}^{5} m_i\Delta_i e^{-m_i x_3},\ \ \widehat{u}_3 = -\frac{1}{\Delta}\sum_{i=1}^{3} m_i\Delta_i e^{-m_i x_3} - \frac{i\xi_1}{\Delta}\sum_{i=4}^{5}\Delta_i e^{-m_i x_3} \quad (31)$$

$$\widehat{t}_{33} = \frac{1}{\Delta}\sum_{i=1}^{5} a_{1i}\Delta_i e^{-m_i x_3},\quad \widehat{t}_{31} = \frac{1}{\Delta}\sum_{i=1}^{5} a_{2i}\Delta_i e^{-m_i x_3},\quad \widehat{m}_{32} = \frac{1}{\Delta}\sum_{i=1}^{5} a_{3i}\Delta_i e^{-m_i x_3}\ , \quad (32)$$

$$\widehat{T} = \frac{1}{\Delta}\sum_{i=1}^{3} R_i^*\Delta_i e^{-m_i x_3},\quad \widehat{P} = \frac{1}{\Delta}\sum_{i=1}^{3} S_i^*\Delta_i e^{-m_i x_3}\ , \quad (33)$$

Here,

$$\Delta = (S_2^*R_1^* - S_1^*R_2^*)n_1 + (S_1^*R_3^* - S_3^*R_1^*)n_2 + (S_3^*R_2^* - S_2^*R_3^*)n_3,$$
$$n_1 = a_{13}a_{24}a_{35} - a_{13}a_{34}a_{25} - a_{14}a_{23}a_{35} + a_{14}a_{33}a_{25} + a_{15}a_{23}a_{34} - a_{15}a_{33}a_{24},$$
$$n_2 = a_{12}a_{24}a_{35} - a_{12}a_{34}a_{25} - a_{14}a_{22}a_{35} + a_{14}a_{32}a_{25} + a_{15}a_{22}a_{34} - a_{15}a_{32}a_{24},$$
$$n_3 = a_{11}a_{24}a_{35} - a_{11}a_{32}a_{25} - a_{14}a_{21}a_{35} + a_{14}a_{31}a_{25} + a_{15}a_{21}a_{34} - a_{15}a_{31}a_{24},$$
$$a_{1i} = (2r_1 + r_2)m_i^2 - \xi_1^2 r_2 - r_3R_i^* - r_4S_i^*, a_{1j} = 2i\xi_1 r_1 m_j, a_{2i}$$
$$= 2i\xi_1(-r_5m_i^3 + r_1m_i + r_5\xi_1^2 m_i),$$
$$a_{2j} = r_5m_j^4 - r_1m_j^2 - r_1\xi_1^2 - r_5\xi_1^4, a_{3i} = 4i\xi_1 r_5 m_i, a_{3j} = -2r_5(m_j^2 + \xi_1^2), r_1 = \frac{\mu}{\gamma_1 T_o}, r_2 = \frac{\lambda_o}{\gamma_1 T_o},$$
$$r_3 = \frac{\rho c_1^2}{\gamma_1 T_o}, r_4 = \frac{\gamma_2^2 b}{\gamma_1 T_o}, r_5 = \frac{\alpha}{4}\frac{\omega^{*2}}{\gamma_1 T_o c_1^2}, i = 1,2,3, j = 4,5.$$

Putting $[-\hat{F}_1(\xi_1),0,0,\hat{F}_2(\xi_1),\hat{F}_3(\xi_1)]^{tr}$ in i^{th} column of Δ respectively determine $\Delta_i (i = 1,2, \ldots 5)$.

6. Applications

6.1 Uniformly distributed source

$$[\boldsymbol{F_1(x_1), F_2(x_1), F_3(x_1)}] = \begin{cases} \boldsymbol{1 if |x_1| \le a_o} \\ \boldsymbol{0 if |x_1| > a_o} \end{cases}$$

Now applying Laplace and Fourier transforms defined by (21) and putting the values

$$[\hat{F}_1(\xi_1), \hat{F}_2(\xi_1), \hat{F}_3(\xi_1)] = \frac{2Sin(\xi_1 a_o)}{\xi_1}, \xi_1 \neq 0, \quad (34)$$

in Eqs. (31)-(33), resulting expressions are obtained. The geometry of uniformly distributed load is given in Fig. 1(a):

6.2 Linearly distributed source

$$[\boldsymbol{F_1(x_1), F_2(x_1), F_3(x_1)}] = \begin{cases} \boldsymbol{1 - \frac{|x_1|}{a_o} if |x_1| \le a_o} \\ \boldsymbol{0 if |x_1| > a_o} \end{cases}$$

Fourier transform in this case applying on the plane boundary $x_3 = 0$ in dimensionless form is

$$[\hat{F}_1(\xi_1), \hat{F}_2(\xi_1), \hat{F}_3(\xi_1)] = \frac{2[1-cos(\xi_1 a_o)]}{\xi_1^2 a_o}, \quad (35)$$

where $2a_o$ is the non dimensional width of the strip of the source.

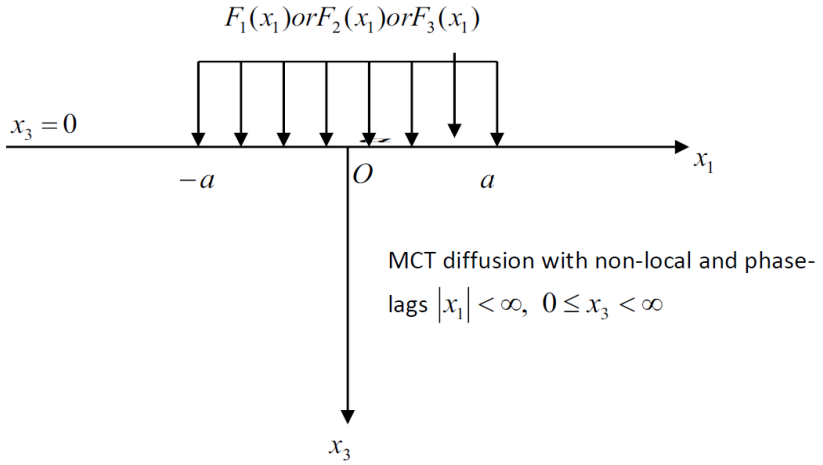

Fig. 1(a) Uniformly distributed normal force $F_1(x_1)$ or uniformly distributed thermal source $F_2(x_1)$ or uniformly distributed chemical potential source $F_3(x_1)$ acting on plane boundary x_3=0

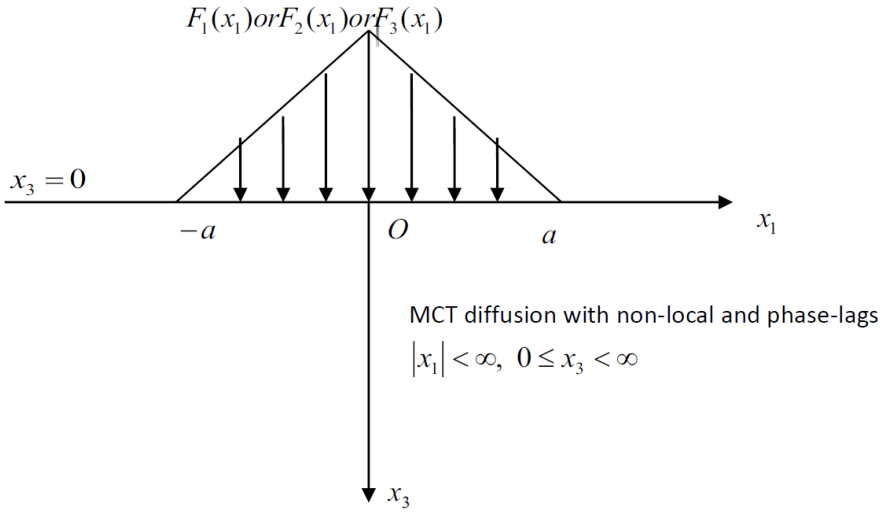

Fig. 1(b) Linearly distributed normal force $F_1(x_1)$ or linearly distributed thermal source $F_2(x_1)$ or linearly distributed chemical potential source $F_3(x_1)$ acting on plane boundary x_3=0

Putting the values from Eq. (35) in Eqs. (31)-(33), resulting expressions are obtained. Complete geometry of linearly distributed load is in Fig. 1(b).

7. Validation

(I) Taking $F_2 = F_3 = 0$ Eqs. (31)-(33) yield the corresponding quantities for normal force.
(II) For thermal source we consider $F_1 = F_3 = 0$ in Eqs. (31)-(33), which in turn yield the required quantities.
(III) Putting $F_1 = F_2 = 0$ in Eqs. (31)-(33) determine the desired quantities for chemical

potential source.

Subcases

(i) Allowing the values of $\hat{F}_1(\xi_1), \hat{F}_2(\xi_1), \hat{F}_3(\xi_1)$ from Eqs. (34) and (35) in Eqs. (31)-(33) gives the resulting expressions for uniformly distributed and linearly distributed normal force respectively.
(ii) Using the values of $\hat{F}_1(\xi_1), \hat{F}_2(\xi_1), \hat{F}_3(\xi_1)$ from Eqs. (34) and (35) in Eqs. (31)-(33) yield the corresponding expressions for uniformly distributed and linearly distributed thermal source respectively.
(iii) Resulting expressions for uniformly distributed and linearly distributed chemical potential source are obtained by substituting the values of $\hat{F}_1(\xi_1), \hat{F}_2(\xi_1), \hat{F}_3(\xi_1)$ from Eqs. (34) and (35) in Eqs. (31)-(33).

Special cases

(1) Taking $\xi = \zeta = \varsigma = 0$ in Eqs. (31)-(33), determine the desired expressions in absence of non-local parameters.
(2) Using $\tau_t = \tau_q = \tau_u = \tau_p = 0$ in Eqs. (31)-(33), determine the desired expressions without dual-phase-lag.

8. Inversion of the transformation

We invert the transforms in Eqs. (31)-(33), with the help of Kumar *et al*. (2017).

9. Numerical implementation and discussion

For numerical computations, following Sherief and Saleh (2005), we take the copper material (thermoelastic diffusion solid) as:

$$\lambda = 7.76 \times 10^{10} Kgm^{-1}s^{-2}, \mu = 3.86 \times 10^{10} Kgm^{-1}s^{-2}, T_o = 0.293 \times 10^3 K, C_e = 0.3891 \times 10^3$$
$$JKg^{-1}K^{-1}, \alpha_t = 1.78 \times 10^{-5}K^{-1}, \alpha_c = 1.98 \times 10^{-4}m^3Kg^{-1}, a = 1.02 \times 10^4 m^2 s^{-2}K^{-1},$$
$$b = 9 \times 10^5 Kg^{-1}m^5 s^{-2}, D = 0.85 \times 10^{-8} Kgm^{-3}s, \rho = 8.954 \times 10^3 Kgm^{-3}, K = 0.386 \times 10^3$$
$$Wm^{-1}K^{-1}, \alpha = 0.05 Kgms^{-2}, t = 0.01s, t_o = 0.2s, \tau_t = 0.6s, \tau_q = 0.7s, \tau_p = 0.8s, \tau_u = 0.9s,$$
$$\xi = 0.395 \times 10^{-9}m, \zeta = 0.2 \times 10^{-9}m, \varsigma = 0.15 \times 10^{-9}m, a_o = 1$$

The software Matlab (R2016a) is used for computation for the following cases:
I. MCT diffusion with non-local and dual-phase-lag (MNP).
II. MCT diffusion with dual-phase-lag (MP).
III. MCT diffusion with non-local and without diffusion phase-lag (MNWDP).
IV. MCT diffusion with non-local and without thermal phase-lag (MNWTP).
V. MCT diffusion with non-local (MN).
Figs. 2-13 are for UDS and figs. 14-25 are for LDS.

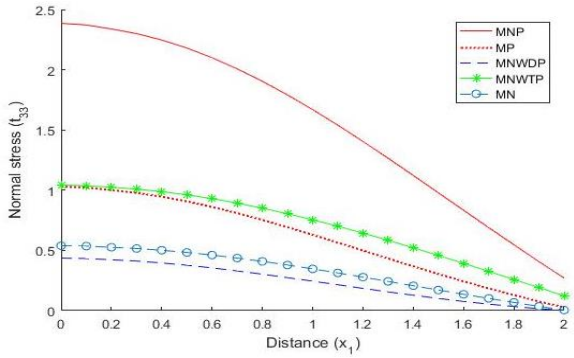

Fig. 2 Profile of t_{33} vs. x_1

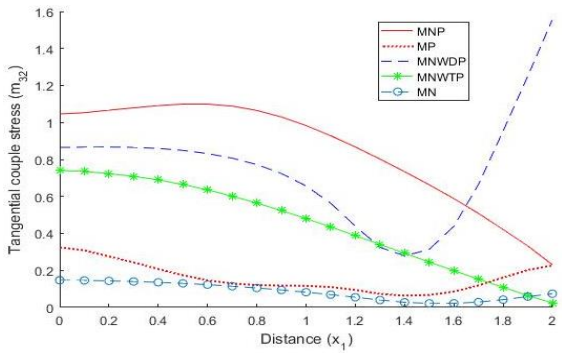

Fig. 3 Profile of m_{32} vs. x_1

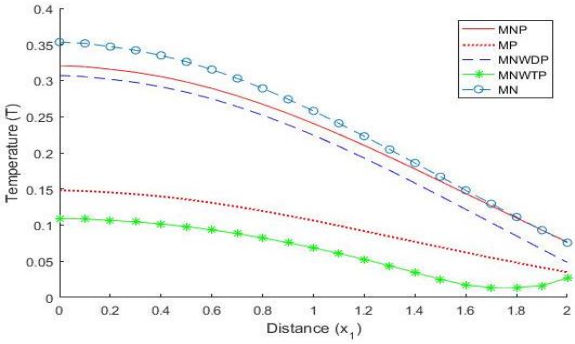

Fig. 4 Profile of T vs. x_1

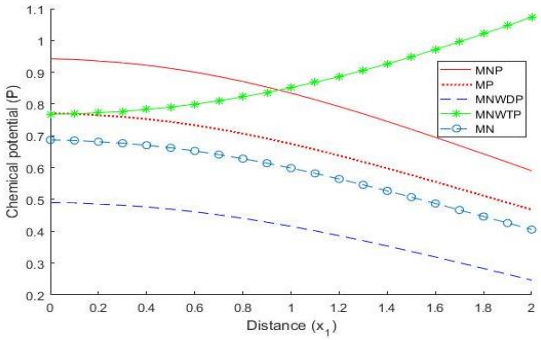

Fig. 5 Profile of P vs. x_1

9.1 Uniformly distributed normal force

Fig. 2 demonstrates trend of t_{33} vs. x_1. t_{33} shows decreasing trend for all the cases. Magnitude of t_{33} for MNP is higher than that for other cases.

Fig. 3 shows trend of m_{32} vs. x_1. Magnitude of m_{32} increases near the source and after that decreases for MNP. m_{32} decrease monotonically for $0 \leq x_1 < 1.5$ and after that increase for MNWDP & MN. m_{32} shows oscillatory behavior for MP and decreasing trend for MNWTP.

Fig. 4 depicts trend of T vs. x_1. T shows decreasing trend for all the cases except for MNWTP far away from the source where it shows increasing trend.

Fig. 5 depicts trend of P vs. x_1. Value of P shows increasing trend for MNWTP and decreasing trend for all the remaining cases with difference in magnitude values.

9.2 Uniformly distributed thermal source

Fig. 6 demonstrates trend of t_{33} vs. x_1. t_{33} shows decreasing trend for all the cases except for MNWTP for which it shows increasing trend.

Fig. 7 shows trend of m_{32} vs. x_1. m_{32} shows decreasing trend for $0 \leq x_1 < 1.2$ and after that increasing trend for MNP, MNWDP and MP. Magnitude of m_{32} decreases near the source and after that fluctuates for MN whereas it decreases monotonically for MNWTP.

Fig. 8 depicts trend of T vs. x_1. Value of T increases with increasing distance for MNWTP and

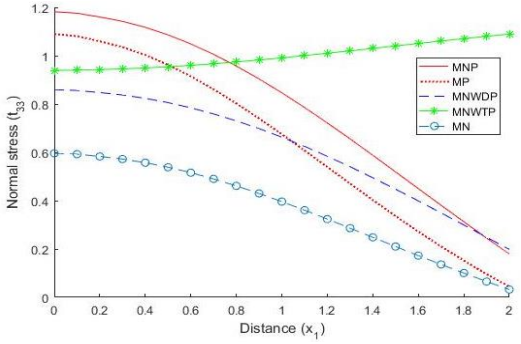

Fig. 6 Profile of t_{33} vs. x_1

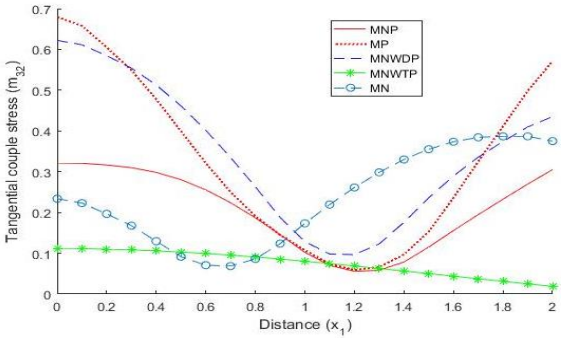

Fig. 7 Profile of m_{33} vs. x_1

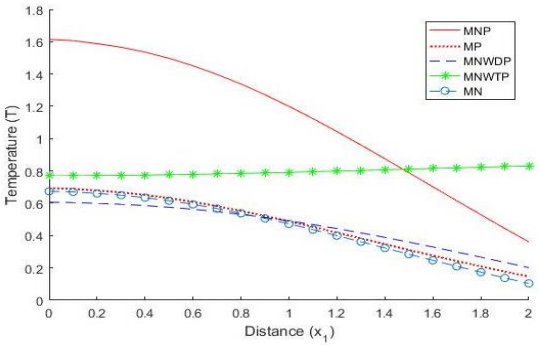

Fig. 8 Profile of T vs. x_1

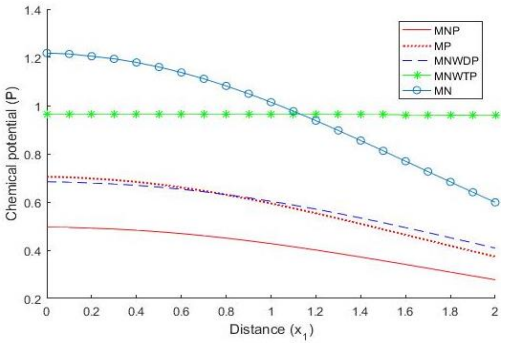

Fig. 9 Profile of P vs. x_1

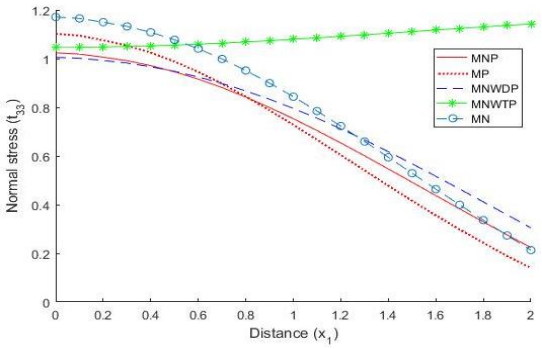

Fig. 10 Profile of t_{33} vs. x_1

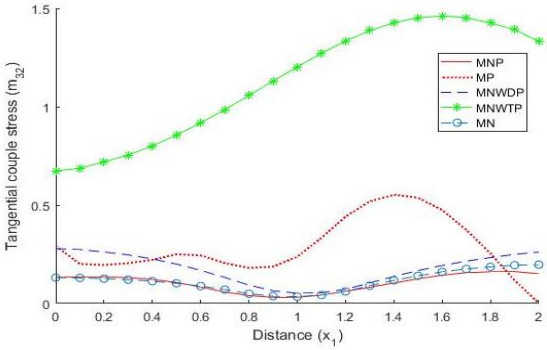

Fig. 11 Profile of m_{32} vs. x_1

decreases for other cases.

Fig. 9 depicts trend of P vs. x_1. Magnitude of P decreases with increasing distance for all the cases except for MNWTP for which it increases.

9.3 Uniformly distributed chemical potential source

Fig. 10 demonstrates trend of t_{33} vs. x_1. Variational behavior of t_{33} is increasing for MNWTP and decreasing for other cases. Behavior of t_{33} is similar for MN & MP.

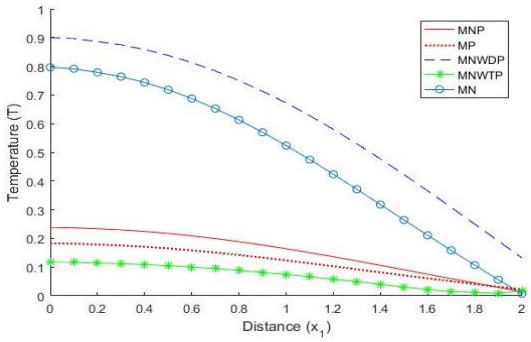

Fig. 12 Profile of T vs. x_1

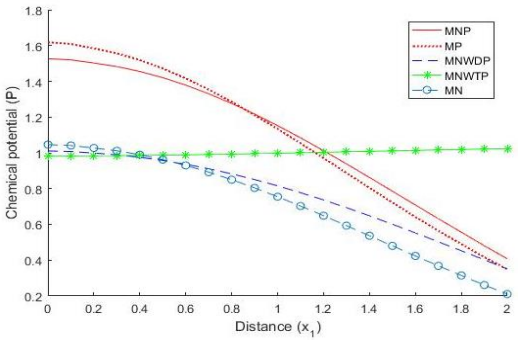

Fig. 13 Profile of P vs. x_1

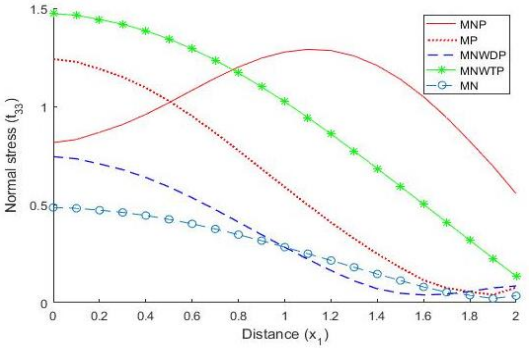

Fig. 14 Profile of t_{33} vs. x_1

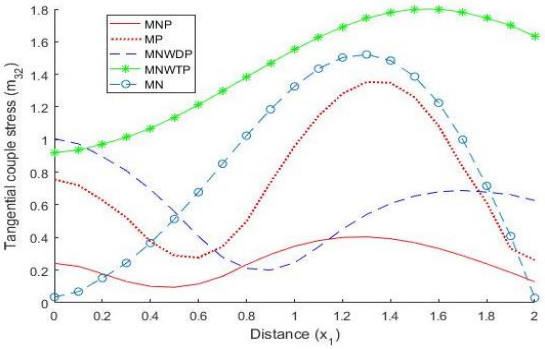

Fig. 15 Profile of m_{32} vs. x_1

Fig. 11 shows trend of m_{32} vs. x_1. Magnitude of m_{32} decrease monotonically for $0 \leq x_1 < 1.0$ and after that increase for MNP, MNWDP and MN. m_{32} shows increasing trend for $0 \leq x_1 < 1.6$ and after that decreasing trend for MNWTP. m_{32} shows oscillatory behavior for MP.

Fig. 12 depicts trend of T vs. x_1. Variational behavior of T is decreasing for all values of x_1 for all the cases with difference in magnitude values. Magnitude of T for MNWDP is higher than the other cases.

Fig. 13 depicts the trend of P vs. x_1. P demonstrates decreasing trend for all the cases except for MNWTP for which it shows monotonically increasing trend.

9.4 Linearly distributed normal force

Fig. 14 demonstrates trend of t_{33} vs. x_1. t_{33} depicts increasing trend for $0 \leq x_1 < 1.2$ and after that increasing trend for MNP. Magnitude of t_{33} decreases with increasing distance for MNWTP. Magnitude of t_{33} decreases for $0 \leq x_1 < 1.2$ and after that increases for remaining cases.

Fig. 15 shows trend of m_{32} vs. x_1. m_{32} demonstrates decreasing trend near the source and after that oscillatory behavior for MNP, MP and MNWDP. m_{32} shows increasing trend for bounded region and after that decreasing trend for MNWTP & MN.

Fig. 16 depicts trend of T vs. x_1. Variational behavior of T is decreasing for all the cases except far away from the source for MNWTP where it shows increasing trend.

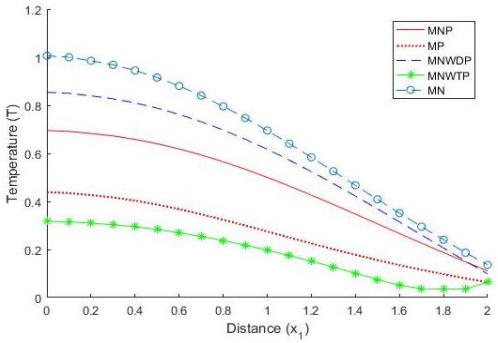

Fig. 16 Profile of T vs. x_1

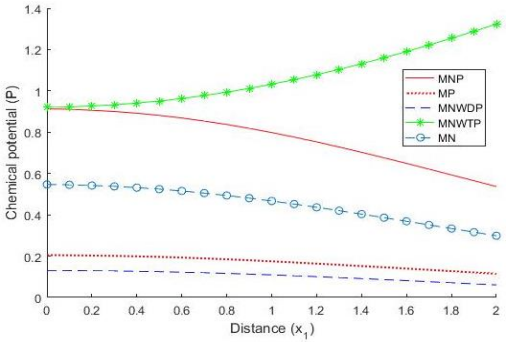

Fig. 17 Profile of P vs. x_1

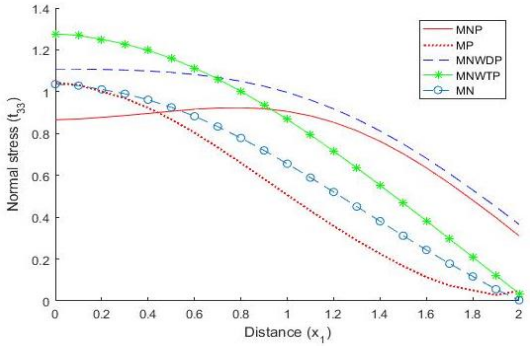

Fig. 18 Profile of t_{33} vs. x_1

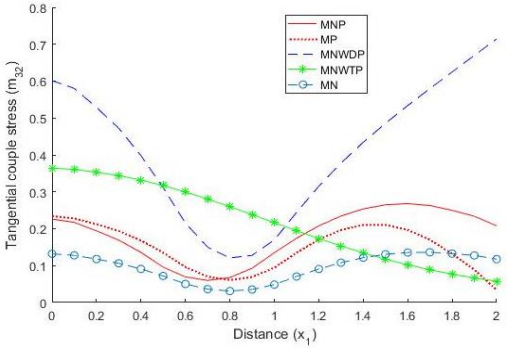

Fig. 19 Profile of m_{32} vs. x_1

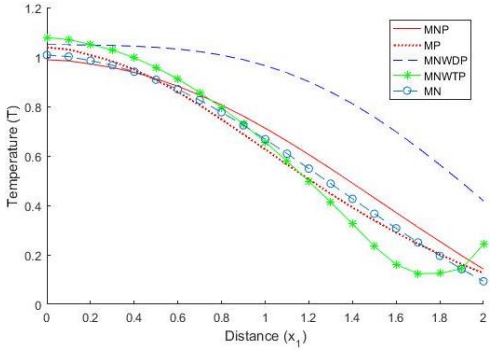

Fig. 20 Profile of T vs. x_1

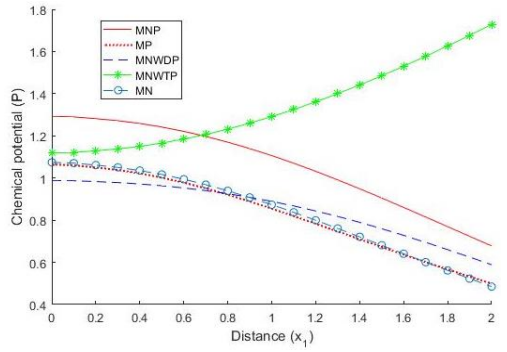

Fig. 21 Profile of P vs. x_1

Fig. 17 depicts trend of P vs. x_1. Magnitude of P monotonically increases for MNWTP and decreases monotonically for all the remaining cases.

9.5 Linearly distributed thermal source

Fig. 18 demonstrates trend of t_{33} vs. x_1. Magnitude of t_{33} increases monotonically for $0 \leq x_1 < 1.0$ and after that decreases for MNP. Variational behavior of t_{33} is decreasing for all the remaining cases.

Fig. 19 shows the trend of m_{32} vs. x_1. Variational behavior of m_{32} is similar for MNP, MN and MN. Values of m_{32} decrease near the source and increase away from the source for MNWDP. Trend of m_{32} is decreasing for MNWTP.

Fig. 20 depicts trend of T vs. x_1. T demonstrates decreasing trend for all the cases except for MNWTP for $x_1 > 1.8$ where it shows increasing trend.

Fig. 21 depicts trend of P vs. x_1. Trend of P is increasing for MNWTP. Magnitude of P decreases with increasing distance for other cases.

9.6 Lineraly distributed chemial potential source

Fig. 22 demonstrates trend of t_{33} vs. x_1. Value of t_{33} increases monotonically for $0 \leq x_1 < 1.0$ and after that decreases for MNP. Variational behavior of t_{33} is decreasing for remaining cases.

Fig. 23 shows the trend of m_{32} vs. x_1. Value of m_{32} is decreasing monotonically for $0 \leq x_1 < 1.0$ and after that increasing for MNP & MNWTP. Magnitude of m_{32} is increasing monotonically except far away from the source where it decreases for MNWDP. m_{32} shows oscillatory behavior for MP & MN.

Fig. 24 depicts trend of T vs. x_1. T demonstrates decreasing trend with increasing distance for all the cases with difference in magnitude values.

Fig. 25 depicts the trend of P vs. x_1. P shows decreasing trend for $x_1 < 1.0$ and increasing trend after that for MNWDP. Magnitude of P decreases monotonically for the remaining cases.

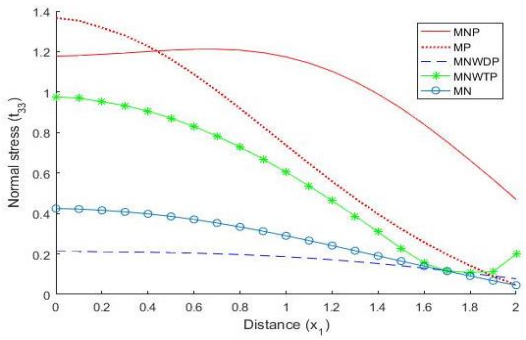

Fig. 22 Profile of t_{33} vs. x_1

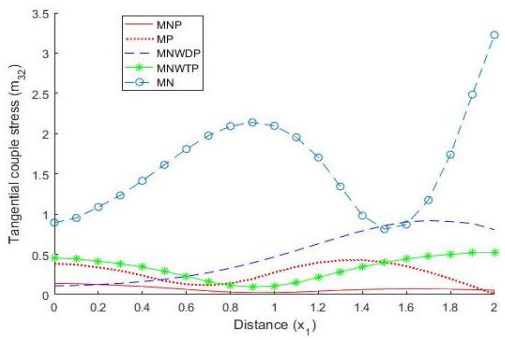

Fig. 23 Profile of m_{32} vs. x_1

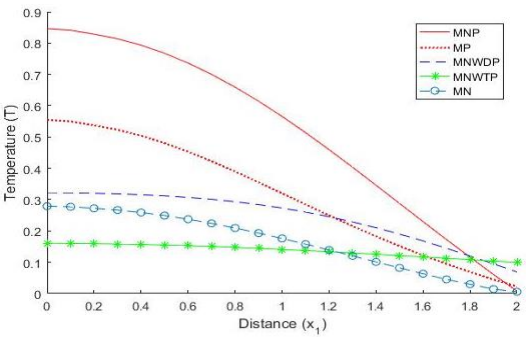

Fig. 24 Profile of T vs. x_1

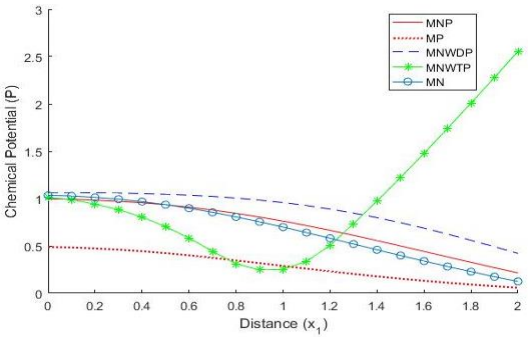

Fig. 25 Profile of P vs. x_1

10. Conclusions

In this problem, thermomechanical load is taken to study the non-local and phase-lags effects in a MCT half space. Laplace transform with respect to time and Fourier transform with respect to space variable are employed to investigate the problem. Thermomechanical loading is classified as UDS and LDS. Inconsistent/non-uniform pattern of curves is followed by the resulting quantities for uniformly distributed normal force. For uniformly distributed thermal source irregular behavior is shown by the resulting quantities. Tangential couple stress shows oscillatory behavior and other quantities show decreasing trend except for MNWTP for normal force and chemical potential for which increasing trend is observed for uniformly distributed chemical potential source.

Fluctuations in the magnitude values of stress components are observed while temperature distribution and chemical potential except for MNWTP show decreasing trend with increasing distance for linearly distributed normal force. Inconsistent/non-uniform pattern of curves is followed by resulting quantities for linearly distributed thermal source. Stress components and temperature follow oscillatory path while temperature distribution and chemical potential shows decreasing trend except for MNWTP for linearly distributed chemical potential source. It is observed that magnitude values of resulting quantities are high in case of UDS in comparison to LDS. The present work is useful for researchers working in modified couple stress thermoelastic with non-local and mass diffusion.

References

Abbas, I.A. and Marin, M. (2018), "Analytical solutions of a two-dimensional generalised thermoelastic diffusion problem due to laser pulse", *Iran. J. Sci. Technol.: Tran. Mech. Eng.*, **42**(3), 57-71. https://doi.org/10.1007/s40997-017-0077-1.

Abouelregal, A.E. and Zenkour, A.M. (2014), "Effect of phase lags on thermoelastic functionally graded microbeams subjected to ramp-type heating", *Iran. J. Sci. Technol.: Tran. Mech. Eng.*, **38**(M2), 321-335. https://doi:10.22099/IJSTM.2014.2498.

Borjalilou, V., Asghari, M. and Taati, E. (2020), "Thermoelastic damping in nonlocal nanobeams considering dual phase lagging effect", *J. Vib. Control*, **26**(11-12), 1-12. https://doi.org/10.1177%2F1077546319891334.

Cao, B.Y. and Guo, Z.Y. (2007), "Equation of motion of a phonon gas and non-Fourier heat conduction", *J. Appl. Phys.*, **5**, 053503. https://doi.org/10.1063/1.2775215.

Edelen, D.G.B. and Laws, N. (1971), "On the thermodynamics of systems with nonlocality", *Arch. Rat. Mech. Anal.*, **43**, 24-35. https://doi.org/10.1007/BF00251543.

Eringen, A.C. (1972a), "On nonlocal fluid mechanics", *Int. J. Eng. Sci.*, **10**(6), 561-575. https://doi.org/10.1016/0020-7225(72)90098-5.

Eringen, A.C. (1972b), "Nonlocal polar elastic continua", *Int. J. Eng. Sci.*, **10**, 1-16. https://doi.org/10.1016/0020-7225(72)90070-5.

Eringen, A.C. (1981), "Nonlocal continuum theory of liquid crystals", *Molecul. Crystal. Liquid Crystal.*, **75**(1), 321-343. https://doi.org/10.1080/00268948108073623.

Eringen, A.C. (1991), "Memory dependent nonlocal electromagnetic elastic solids and superconductivity", *J. Math. Phys.*, **32**(3), 787-796. https://doi.org/10.1063/1.529372.

Eringen, A.C. (2002), *Nonlocal Continuum Field Theories*, Springer, New York, United States.

Eringen, A.C. and Edelen, D.G.B. (1972), "On nonlocal elasticity", *Int. J. Eng. Sci.*, **10**(3), 233-248. https://doi.org/10.1016/0020-7225(72)90039-0.

Guo, Z.Y. and Hou, Q.W. (2010), "Thermal wave based on the thermomass model", *J. Heat Transf.*, **7**,

072403. https://doi.org/10.1115/1.4000987.
Kumar, R. and Abbas, I.A. (2016), "Disturbance due to thermomechanical sources in porothermoelastic medium", *Strength Mater.*, **48**(2), 315-322. http://doi.org/10.1007/s11223-016-9767-y.
Kumar, R., Devi, S. and Sharma V. (2017), "Effect of hall current and rotation in modified couple stress generalised thermoelastic half space due to ramp type heating", *J. Solid Mech.*, **9**(3), 527-542.
Kumar, R., Devi, S. and Sharma, V. (2019), Resonance of nanoscale beam due to various sources in modified couple stress thermoelastic diffusion with phase lags", *Mech. Mech. Eng.*, **23**(1), 36-49. http://doi.org/10.2478/mme-2019-0006.
Kumar, R., Miglani, A. and Rani, R. (2018), "Transient analysis of nonlocal microstretch thermoelastic thick circular plate with phase lags", *Mediterran. J. Model. Simul.*, **9**, 25-42.
Marin, M., Abbas, I.A. and Kumar, R. (2014), "Relaxed Saint-Venant principle for thermoelastic micropolar diffusion", *Struct. Eng. Mech.*, **51**(4), 651-662. http://doi.org/10.12989/sem.2014.51.4.651.
Mashat, D.S. and Zenkour, A.M. (2020), "Modified DPL Green-Naghdi theory for thermoelastic vibration of temperature dependent nanobeams", *Result. Phys.*, **16**, 102845. https://doi.org/10.1016/j.rinp.2019.102845.
Sharma, K. (2012), "Reflection of plane waves in thermodiffusive elastic half space with voids", *Multidisc. Model. Mater. Struct.*, **8**(3), 269-296. https://doi.org/10.1108/15736101211269113.
Sharma, S. and Sharma, K. (2014), "Influence of heat sources and relaxation time on temperature distribution in tissues", *Int. J. Appl. Mech. Eng.*, **19**(2), 427-433. http://doi.org/10.2478/ijame-2014-0029.
Sherief, H.H. and Saleh, H. (2005), "A half space problem in the theory of generalised thermoelastic diffusion", *Int. J. Solid. Struct.*, **42**(15), 4484-4493. https://doi.org/10.1016/j.ijsolstr.2005.01.001.
Sherief, H.H., Hamza, F.A. and Saleh H.A. (2004), "The theory of generalised thermoelastic diffusion", *Int. J. Eng. Sci.*, **42**(5-6) 591-608. https://doi.org/10.1016/j.ijengsci.2003.05.001.
Tzou, D.Y. (1992), "Thermal shock phenomena under high rate response in solids", *Ann. Rev. Heat Transf.*, **4**, 111-185. https://doi.org/10.1615/ANNUALREVHEATTRANSFER.V4.50.
Tzou, D.Y. (1995a), "A unified field approach for heat conduction from macro to micro scales", *J. Heat Transf.*, **117**(1), 8-16. https://doi.org/10.1115/1.2822329.
Tzou, D.Y. (1995b), "The generalised lagging response in small scale and high rate heatng", *Int. J. Heat Mass Transf.*, **38**(17), 3231-3240. https://doi.org/10.1016/0017-9310(95)00052-B.
Tzou, D.Y. and Guo, Z.Y. (2010), "Nonlocal behavior in thermal lagging", *Int. J. Therm. Sci.*, **49**(7), 1133-1137. https://doi.org/10.1016/j.ijthermalsci.2010.01.022.
Yu, J., Tian, X.G. and Xiong, Q.L. (2016), "Nonlocal thermoelasticity based on nonlocal heat conduction and nonlocal elasticity", *Eur. J. Mech.-A/Solid.*, **60**, 238-253. http://doi.org/10.1016/j.euromechsol.2016.08.004.
Zhang, L., Bhatti, M.M., Marin, M. and S. Makheimer, K. (2020), "Entropy analysis on the blood flow through anisotropically tapered arteries filled with magnetic zinc-oxide nanoparticles", *Entropy*, **22**, 1070. https://doi.org/10.3390/e22101070.